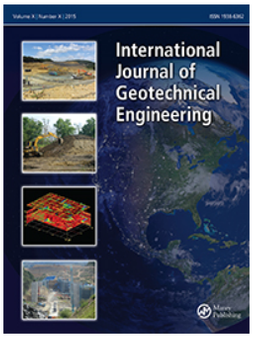

International Journal of Geotechnical Engineering

ISSN: 1938-6362 (Print) 1939-7879 (Online) Journal homepage: http://www.tandfonline.com/loi/yjge20

Soft soils improvement by granular piles reinforced with horizontal geogrid strips

Murtaza Hasan & N. K. Samadhiya

To cite this article: Murtaza Hasan & N. K. Samadhiya (2016): Soft soils improvement by granular piles reinforced with horizontal geogrid strips, International Journal of Geotechnical Engineering, DOI: 10.1080/19386362.2016.1252139

To link to this article: http://dx.doi.org/10.1080/19386362.2016.1252139

Published online: 17 Nov 2016.

Soft soils improvement by granular piles reinforced with horizontal geogrid strips

Murtaza Hasan* and N. K. Samadhiya

The present paper investigates the effect of geogrid, as horizontal strips, on the ultimate load intensity and bulging of floating as well as end bearing granular piles. The laboratory model tests and numerical analyses have been carried out on unreinforced and granular piles reinforced with horizontal geogrid strips embedded in very soft clay. The short-term and displacement controlled laboratory model tests were carried out based on unit cell concept. Numerical analysis has been extended to study the influence of shear strength of clay, number and stiffness of geogrid strips on the granular piles. The results of laboratory model tests in the form of load–settlement relationship were compared with those obtained from FEM software, PLAXIS 3D. The ultimate load intensity for unreinforced floating and end bearing granular piles treated ground has been increased by 185 and 238% as compared to untreated ground. The ultimate load intensity for 25, 50 and 70 mm c/c spaced floating granular piles reinforced with horizontal strips-treated ground increased by 442, 396 and 316% as compared to untreated ground. The results indicated significant improvement in the ultimate load intensity and reduction in bulging of granular piles by incorporating geogrid strips.

Keywords: Stone columns, Geogrid, Plaxis 3D, Soft clays, Numerical analysis

Introduction

The granular piles (also known as stone columns) have been widely adopted in soft soils to increase carrying capacity as one the of several ground improvement techniques available. It also increases the rate of consolidation and reduces settlements. The granular piles have been successfully provided below embankments, liquid storage tanks, raft foundations and other low rise structures. The improvement depends on the lateral confining pressure from soil surrounding the granular piles. In very soft clays, granular piles do not achieve significant load-carrying capacity, so additional confinement is needed for its better performance. In recent years, geosynthetic has been successfully used in granular piles installed in very soft clays, in the form of vertical encasing or in horizontal layers to provide additional confinement. Vertical encased granular piles have several advantages such as increment in load-carrying capacity of pile by mobilisation of hoop stress in reinforced material; preventing the loss of aggregates into surrounding soft clay; preserving the drainage and frictional properties of the stone aggregates. In the past, various researchers such as Murugesan and Rajagopal (2006, 2007), Gniel and Bouazza (2009), Wu and Hong (2009), Pulko *et al.* (2011), Ali *et al*. (2012), Yoo and Lee (2012), Ghazavi and Afshar (2013), Almeida *et al*. (2014), Zhang and Zhao (2015), Mohapatra *et al*. (2016) and Hasan and Samadhiya (2016) have conducted large- and small-scale laboratory tests, numerical analysis and field tests on vertical encased granular piles in very soft clays. Granular piles reinforced with horizontal strips (GPHS) not only improve load capacity of treated ground but also control bulging by development of shear stress at the strips–stone aggregates interface. Madhav (1982) has performed small-scale *in situ* tests on GPHS. Sharma *et al*. (2004), Ayadat *et al*. (2008) and Ali *et al*. (2012) have conducted laboratory model tests on horizontally striped granular piles, whereas Madhav *et al*. (1994) and Wu and Hong (2008) have given an analytical procedure to predict the response of treated ground with horizontally striped granular piles. The load-carrying capacity of GPHS depends on the number of strips, vertical spacing between the strips and frictional properties of the granular materials as reported by Madhav *et al*. (1994). Sharma *et al*. (2004) presented a series of results of experiments performed to investigate the effect of horizontal geogrid layers on bulging and load-carrying capacity of granular piles in a soft clay bed. Ayadat *et al*. (2008) presented results of an experimental investigation on sand columns reinforced with horizontal wire meshes made of plastic, steel and aluminium materials. They investigated load-carrying capacity of reinforced sand columns and proposed a theoretical model to predict the load-carrying capacity of these columns. Samadhiya *et al*. (2008) investigated the performance of granular piles reinforced with nylon fibres and found that the load-carrying capacity increases with the increase in the length of fibre; fibre content up to 1% and showed declining trend at 2% fibre content. Hong and Wu (2013) carried out numerical analysis and laboratory triaxial compression tests on

Department of Civil Engineering, Indian Institute of Technology Roorkee, Roorkee 247667, India

*Corresponding author, email hasandce@iitr.ac.in

Received 10 August 2016; accepted 18 October 2016
DOI 10.1080/19386362.2016.1252139

sand columns internally reinforced with horizontal geotextile layers. They compared numerical and experimental results in the form of deviatoric stresses and volumetric strains.

Enough literature is not available on assessment of improvement in the load-carrying capacity of the floating GPHS. The numerical analysis has not been reported enough in the literature on floating and end bearing GPHS installed in very soft clays. In the present study, laboratory model tests and numerical analyses have been carried out on both floating and end bearing GPHS. Numerical analysis has been extended to the study effect of length of reinforcement, undrained shear strength of clay and geogrid stiffness using Finite-element analysis (FEM) software, PLAXIS 3D. The assessment of ultimate load intensity and bulging of granular piles were investigated.

Experimental programme

The experimental programme consisted of laboratory model tests on clay bed, unreinforced granular piles (URGP) and GPHS. The unit cell idealisation was adopted by assuming piles in a triangular pattern. It is widely used to simplify the design of the apparatus needed to assess the behaviour of an interior granular pile when the piles in large groups are simultaneously loaded. Various researchers such as Barksdale and Bachus (1983), Murugesan and Rajagopal (2007), Ambily and Gandhi (2007) and Mohanty and Samanta (2015) have used unit cell concept in their experimental investigations. The laboratory model tests were carried out on 75 mm diameter single floating and end bearing granular piles installed in soft clay. The cylindrical tank of 200 mm diameter and 525 mm height was used to prepare the clay bed. The length of granular piles was kept 5*d* (375 mm) for floating piles and 7*d* (525 mm) for end bearing piles, where *d* is the diameter of the pile. The area replacement ratio, A_r (ratio of the area of the granular pile to the total area within the unit cell) was kept 14%. Undrained shear strength (c_u) of the soft clay was kept close to 5 kPa throughout the experimental work. Sharma *et al*. (2004) and Ghazavi and Afshar (2013) reported in the literature that the ultimate capacity of granular pile increases with increase in the depth of encasement, and with an increase in the number of geogrid horizontal strips. Therefore, circular geogrid strips of 65 mm diameter were used over the entire length of granular piles. These strips were placed at three different centres to centre spacing (*S*) of 25 mm (*d/3*), 50 mm (*2d/3*) and 70 mm (≈*d*). First geogrid strip in each case was placed 25 mm below the top of the granular pile. The parameters included in this investigation are strips spacing, undrained shear strength of clay, length of reinforcement (number of strips) and geogrid stiffness.

Materials properties

The dried clay classified as CI as per IS: 1498 (2000) was converted into fine powder by grinding and stored in air dried room. The physical properties of clay are presented in Table 1. The crushed granite aggregates used to construct granular piles were in the range of 2–6.3 mm in size. The maximum and minimum dry unit weights of the aggregate are 15.04 and 13.41 kN/m^3, respectively. The relative density of stone aggregates was considered 70% to ensure negligible bulging during construction of pile. Corresponding dry unit weight and angle of internal friction of stone aggregates are 14.51 kN/m^3 and 43°, respectively. The particle size distribution curves for both clay and crushed stones are shown in Fig. 1.

Biaxial geogrid was used as internal reinforcement in the form of horizontal strips. Thickness and aperture size of geogrid mesh were 3.2 mm and 6 mm × 6 mm respectively. Tensile strength of geogrid was reduced as per scaling laws proposed by Iai (1989). In laboratory model tests, Murugesan and Rajagopal (2007, 2010), Gniel and Bouazza (2009) and Ghazavi and Afshar (2013) have used ultimate tensile strength

Table 1 Physical properties of clay

Properties	Value
Specific gravity	2.73
Optimum moisture content (%)	17.56
Maximum dry unit weight (kN/m^3)	17.22
Liquid limit, w_l (%)	48
Plastic limit, w_P (%)	18
Plasticity index (%)	30
Dry unit weight at 34% water content (kN/m^3)	13.85
Undrained shear strength at 34% water content (kPa)	≈5
Classification	CI

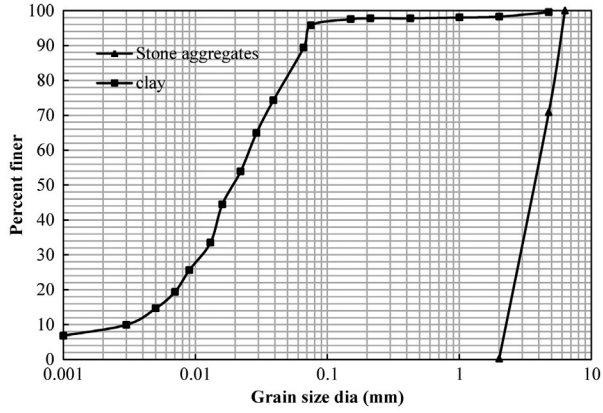

1 Particle size distribution curves for clay and stone aggregates

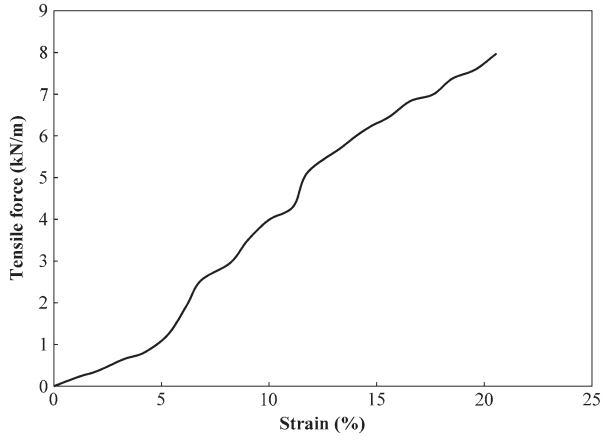

2 Tensile force–strain behaviour of geogrid sample

of geosynthetic in the range of 1.5–20 kN/m. The ultimate tensile strength of geogrid was determined from standard wide-width tension tests as per ASTM D4595 (1986). Tensile force-strain behaviour of geogrid sample is presented Fig. 2. The ultimate tensile strength and axial stiffness of geogrid used in the present study were found to be 7.96 and 38.01 kN/m. The strain corresponding to ultimate tensile force was found to be 20.2%.

Preparation of clay bed

A 525 mm high clay bed was prepared having undrained shear strength close to 5 kPa in the all experiments. The undrained shear strength of clay corresponding to varying moisture contents were determined by performing laboratory unconfined compression tests. The water content and dry unit weight (corresponding to 5 kPa shear strength) were found to be 34% and 13.85 kN/m^3, respectively. The quantity of clay corresponding to dry unit weight was calculated and mixed thoroughly with water (34%) in a large steel container. A thin coat of grease was applied on the inner wall of 200 mm diameter cylindrical tank to minimise friction between clay and inner wall. The tank was filled in layers of 30 mm in height. Each layer was compacted properly. After completion of clay bed, tank was covered with wet jute bag and left for two days to gain uniformity. Vane shear tests were conducted at the centre of clay bed to ensure the required shear strength before construction of granular piles. All vane shear tests have shown shear strength close to 5 kPa. Fresh clay was used in each laboratory test for better control on moisture content.

Construction of granular pile

A 75 mm diameter granular pile was formed using replacement technique in all laboratory model tests. Technique is known to produce the granular piles of excellent consistency. A thin seamless steel pipe of 75 mm outer diameter with the help of auger guide was inserted smoothly in the centre of clay bed up to the desired height of granular pile. Oil was applied on both outer and inner surface of steel pipe to allow easy insertion as well as withdrawal and to avoid sticking of clay to pipe. A 73 mm diameter helical steel auger was used to scoop out clay within the steel pipe. Approximately, 20 mm height of clay was scooped to avoid suction between auger and pipe in a single stroke. Aggregates in predetermined quantity (corresponding to dry unit weight of 14.51 kN/m^3) between two geogrid layers were poured and then light compacted within hole before placing next circular strip. Fresh aggregates were used for each laboratory test for better results.

Test set-up and procedure

Figure 3 shows a schematic view of test set-up for laboratory model tests. The vertical load was applied through a 15 mm thick loading plate at a constant displacement rate of 1.2 mm/min. The load was increased till the plate undergoes 35 mm settlement. The load was applied either only over the cross-sectional area of granular pile or over the entire cross-sectional area of the unit cell. When the entire unit cell area was loaded,

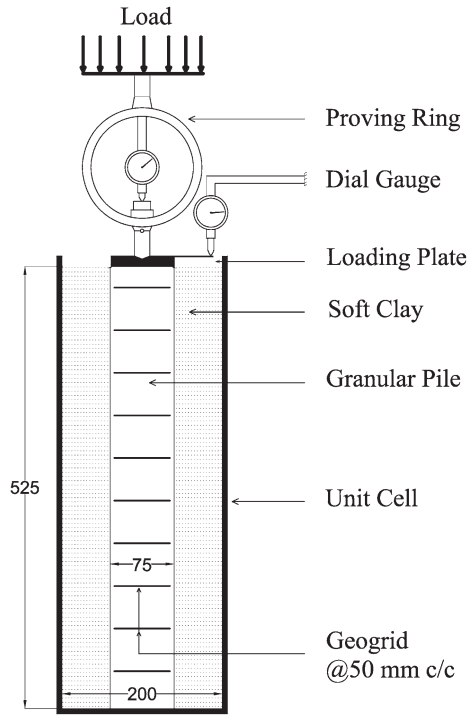

3 Schematic view of test set-up (end bearing GPHS)

the load was applied through a steel plate of diameter 10 mm less than the inside diameter of the test tank. For floating GP, load was applied only over the area of granular pile. In case of end bearing GP, load was applied either only over the area of granular pile or over the entire area of tank. A proving ring and dial gauge were used to measure the applied load and settlement, respectively. The period of loading was kept short to ensure undrained loading condition which simulates loading during construction. Load–settlement behaviour was studied for the assessment of performance of the granular piles. Ultimate load intensity and ultimate bearing capacity of treated ground were evaluated after applying load only on granular piles and entire area respectively. After completion of each test, aggregates were removed and then slurry of plaster of Paris was poured into thus formed hole and allowed to set for 24 h. Surrounding clay was removed carefully and deformed shape of granular pile was obtained and painted in white colour for better visibility to quantify the bulging.

Finite-element analysis

FEM analysis was carried out by finite-element software, PLAXIS 3D. PLAXIS 3D model has been validated by obtaining load–settlement behaviour of granular pile based on laboratory test carried out by Basu (2009). Basu (2009) conducted model test on 0.2625 m × 0.2625 m × 0.6 m tank. The author installed a single 75 mm diameter and 600 mm length granular pile in the centre of tank and loaded with circular plate of equal diameter. Fibre was mixed in the sand to internally reinforce the granular piles. The model was simulated and analysed using Mohr–Coulomb failure criterion. The material properties used in the modelling are given in Table 2. The mesh generated and

Table 2 Material properties for PLAXIS 3D

	Basu (2009)		Present study	
Parameters	Clay	Sand–fibre mix	Clay	Stone aggregates
Young's modulus, E (kPa)	250	6700	420	42500
Cohesion (kPa)	16.0	15.55	As per Table 3	0
Angle of internal friction, ϕ (°)	0	34.47	0	43
Poisson's ratio, μ	0.3	0.3	0.48	0.3
Dry unit weight (kN/m^3)	14.90	18.0	13.85	14.51
Bulk unit weight (kN/m^3)	19.37	–	18.58	–

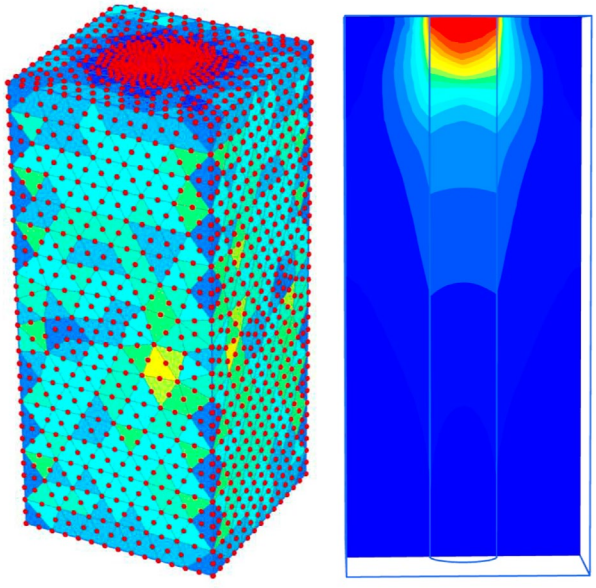

4 Mesh generation and total displacements in model, Basu (2009)

total displacements after model failure are shown in Fig. 4. The comparison of experimental and PLAXIS 3D model results are presented in Fig. 5 and shows a reasonably good agreement.

In the present study, a linear elastic perfectly plastic Mohr–Coulomb model, which also used for similar study by Ambily and Gandhi (2007), Pulko *et al.* (2011), Ghazavi and Afshar (2013), Chen *et al*. (2015) and Mohanty and Samanta (2015), has been adopted for clay and stone aggregates. Geogrid strips were modelled as elastic material. The input parameters (E, c_u, ϕ, γ_d, ψ) were determined from the relevant laboratory tests and are given in Table 2. Modulus of elasticity of soft clay was determined by consolidation test corresponding to a pressure range of 100–200 kPa as reported by Ambily and Gandhi (2007). The Poisson's ratio was taken as per values given by Bowles (1997). The cylindrical unit cell of equivalent diameter was simulated as square unit cell model in the present study. Ng and Tan (2015) investigated that the results in Plaxis

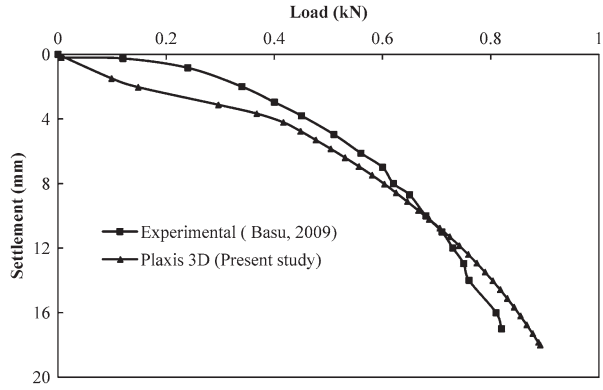

5 PLAXIS validation through experimental result, Basu (2009)

2d and 3d models are similar especially for load–settlement behaviour and failure mechanism. Square unit cell was also simulated by Murugesan and Rajagopal (2006), Ambily and Gandhi (2007) and Mohanty and Samanta (2015). The granular piles experience radial bulging without significant shear on the interface between granular pile and clay as reported by Mitchell and Huber (1985) and Ambily and Gandhi (2007). Therefore, an interface element has not been used in the present study. The generated meshes used for 50 mm spaced horizontal stripped end bearing granular pile models are presented in Fig. 6.

Results and discussion

In the present investigation, the results of laboratory model tests in the form of vertical load–settlement relationship have been compared with those obtained from numerical analyses by FEM software, PLAXIS 3D. The experimental and numerical analysis results in term of load–settlement relationship of clay bed, URGPs (floating and end bearing) are presented in Fig. 7 for the case when only granular piles are loaded. Perusal of Fig. 7 indicated that the results from experimental and numerical study are in close agreement. The results are also summarised in Table 3. The ultimate load intensity of granular piles increased with an increase in the length of pile. The ultimate load intensity for floating and end bearing (URGP) treated ground from laboratory results was found to increase by 185 and 238% as compared to untreated ground. The increment in ultimate load intensity of URGP (end bearing) was found to be 19% as compared to URGP (floating). The floating URGP penetrates into the soft clay upon application of the load whereas end bearing URGP is offered resistance from the tip of pile also. Further, the percentage of soft soils replaced in end bearing GP is more than that in floating GP. Hence, ultimate load intensity of end bearing GP treated ground was found to increase as compared to floating GP. The experimental and FEM results in terms of load–settlement behaviour for floating GPHS with three different spacings are presented in Fig. 8. The ultimate load intensity of granular piles has been found to increase with a reduction in the spacing of geogrid layers. The ultimate load intensity for 25, 50 and 70 mm c/c spaced floating GPHS treated ground was found to increase by 442, 396 and 316% as compared to untreated ground, 89, 73 and 45% with respect to URGP

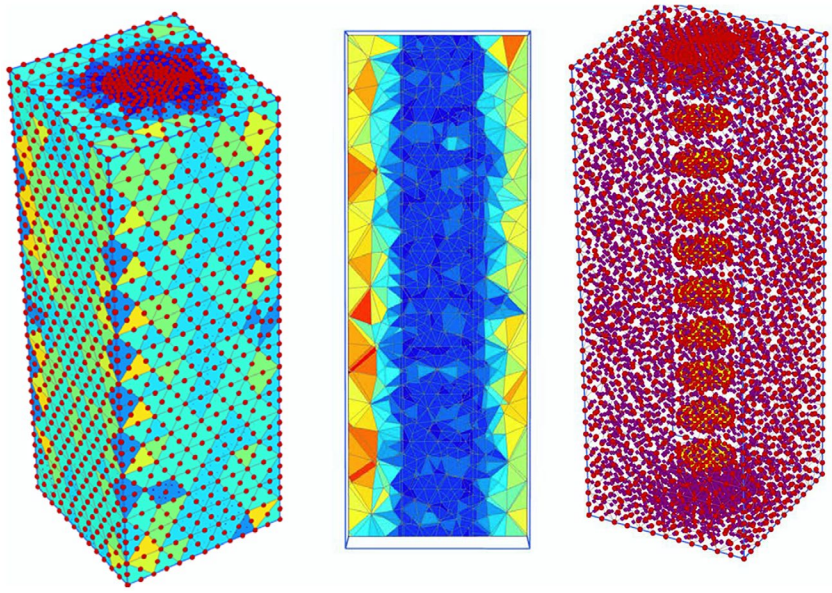

6 Mesh generation end bearing GPHS @ 50 mm c/c

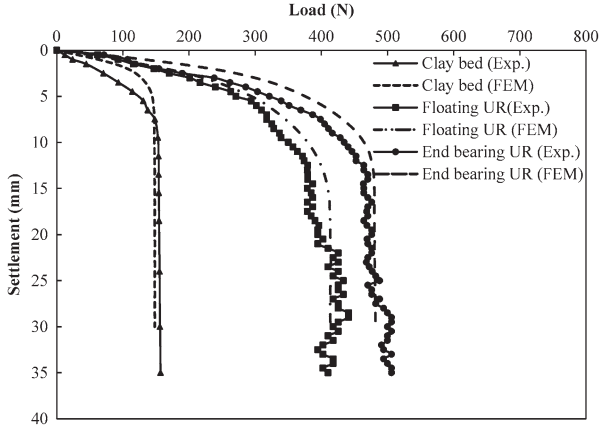

7 Load–settlement relationship of URGPs

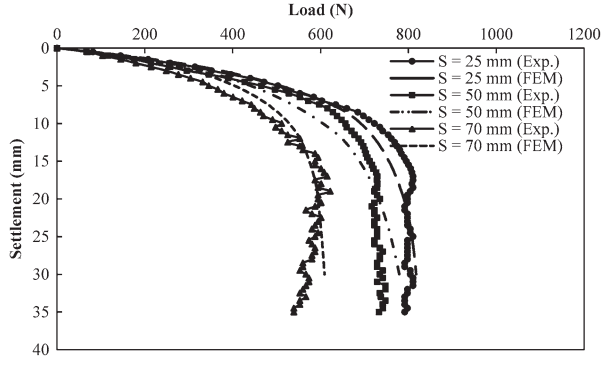

8 Load–settlement behaviour for floating GPHS

Table 3 Results of laboratory model tests and FEM analysis

Test description		Pile alone loaded		
			Ultimate load intensity (kPa)	
Type of piles	Strip spacing (mm)	c_u (kPa)	Exp.	FEM
Clay bed	–	5.12	33.85	33.64
UR floating	–	5.01	96.65	94.87
UR end bearing	–	5.09	114.58	109.08
Floating GPHS	25	5.29	183.55	185.14
	50	5.17	167.90	176.45
	70	5.13	140.86	137.89
End bearing GPHS	25	5.34	218.62	221.72
	50	5.25	202.25	194.39
	70	5.10	148.25	140.83

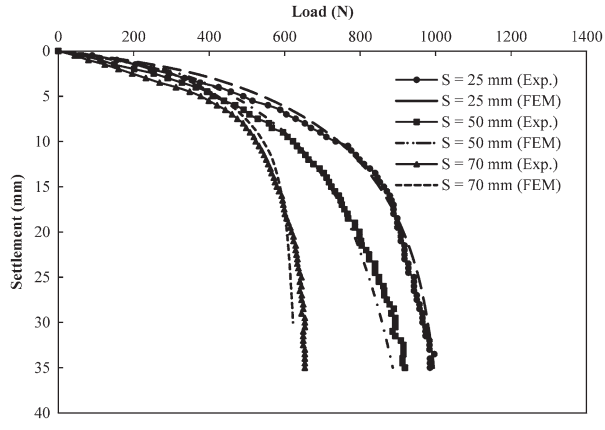

9 Load–settlement behaviour for end bearing GPHS

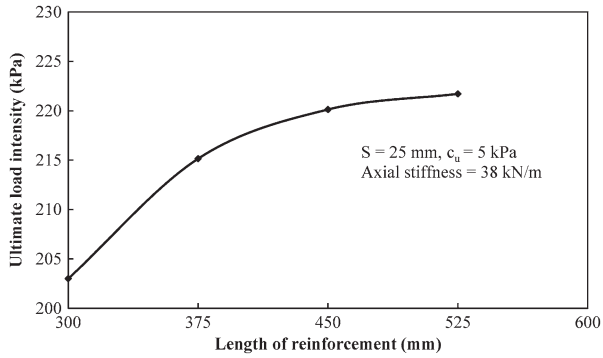

10 Variation of the ultimate load intensity with reinforcement length

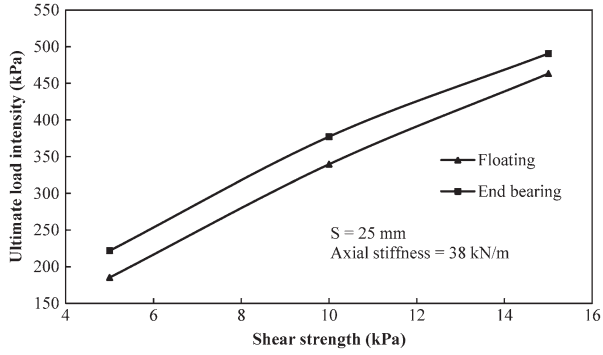

11 Variation of the ultimate load intensity with shear strength

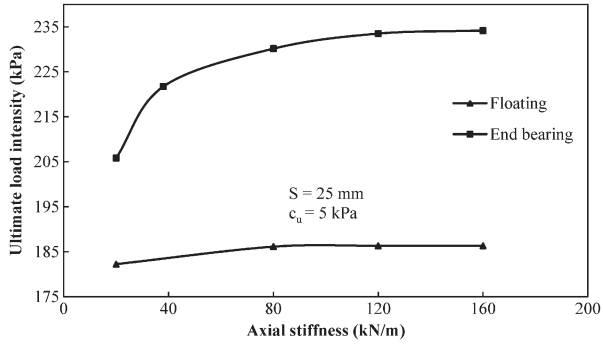

12 Variation of the ultimate load intensity with geogrid stiffness

(floating) and 60, 46 and 22% as compared to URGP (end bearing), respectively. The experimental and FEM results in terms of load–settlement behaviour for end bearing GPHS are presented in Fig. 9. The ultimate load intensity for 25, 50 and 70 mm c/c spaced end bearing GPHS treated ground was found to increase by 545, 497 and 338% as compared to untreated ground, 90, 76 and 29% with respect to URGP (end bearing) and 126, 109 and 53% as compared to URGP (floating), respectively. The horizontal geogrid strips, placed at regular spacing in granular piles improves the ultimate load intensity and control bulging by mobilising friction on the surface of strips surrounding by stone aggregates. Ultimate

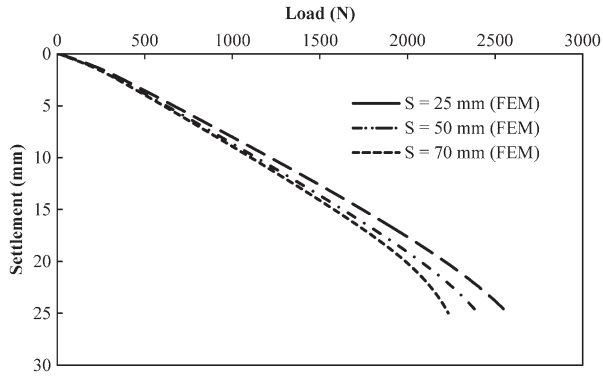

13 Load–settlement behaviour for end bearing GPHS (entire area loaded)

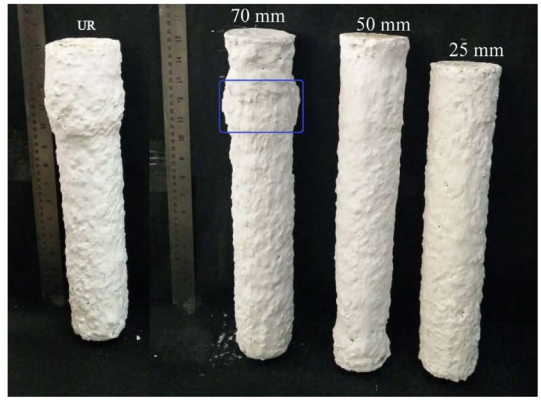

(a)

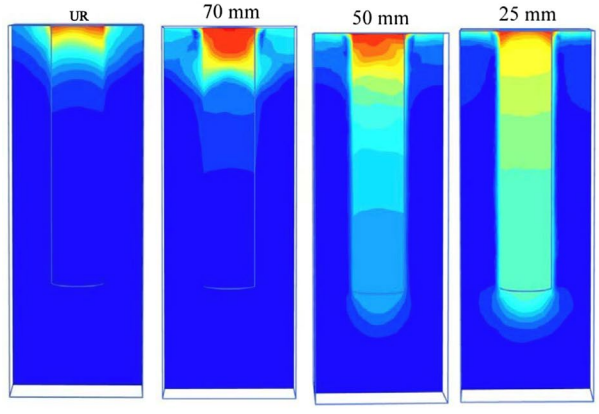

(b)

14 Deformed shapes of floating URGP and GPHS; *a* laboratory model tests, *b* FEM

load intensity of GPHS has been found to increase further as the number of strips adds to the improvement in confining effect on the granular material.

The numerical analysis has been extended to study the influence of length of reinforcement, undrained shear strength of the soft clay and stiffness of geogrid on the ultimate load intensity of GPHS (floating and end bearing). The length of

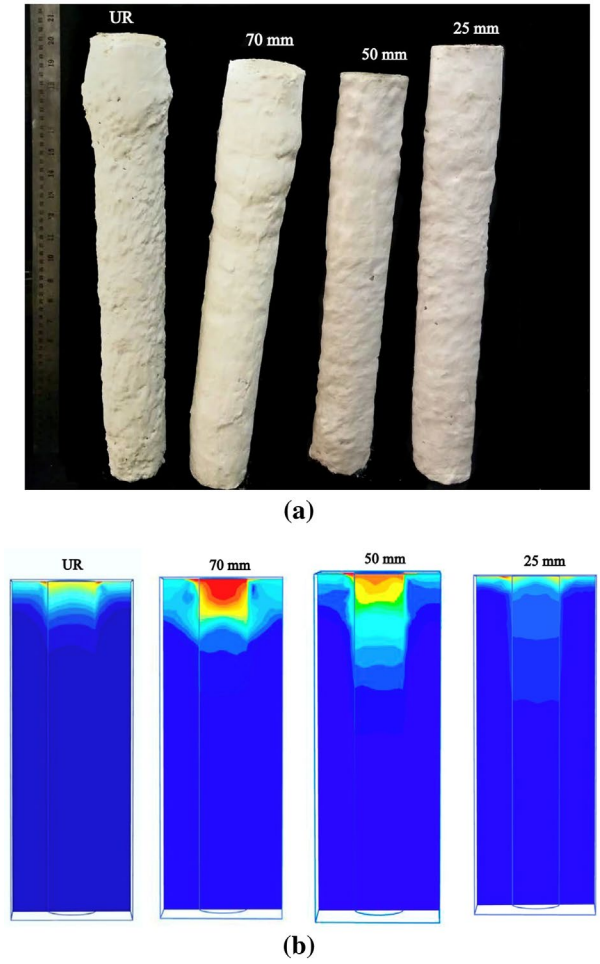

15 Deformed shapes of end bearing URGP and GPHS; *a* laboratory model tests, *b* FEM

reinforcement was varied from 4d to 7d for end bearing piles. The spacing in strips, axial stiffness of geogrid and undrained shear strength of clay were kept as 25 mm, 38 kN/m and 5 kPa, respectively. The variation of ultimate load intensity with length of reinforcement in the GPHS is shown in Fig. 10. The ultimate load intensity of end bearing GPHS-treated ground increased with an increase in the length of reinforcement. Similar trend was also observed by Sharma *et al*. (2004). However, increment in ultimate load intensity was much higher for the length from 4d to 6d as compared to 6d–7d. It may also be noted that end bearing GPHS with strip spacing 25 mm and reinforcement length 300 mm (4d), ultimate load intensity of granular pile was observed higher as compared to end bearing GPHS (strips spacing 50 and 70 mm) with reinforcement up to entire pile length. The undrained shear strength of clay was kept in the range of 5–15 kPa for floating and end bearing GPHS. The spacing in strips (up to entire length of pile) and axial stiffness of geogrid were kept as 25 mm and 38 kN/m, respectively. The variation of ultimate load intensity of GPHS with undrained shear strength of clay is shown in Fig. 11. The ultimate load intensity for GPHS increased with the increase in undrained shear strength of clay. It may be attributed to the higher lateral confinement provided surrounding clay. The axial stiffness of geogrid strips was varied in the range 20–160 kN/m for floating and end bearing GPHS. The spacing in strips (up to entire length of pile) and undrained shear strength of clay were kept as 25 mm and 5 kPa, respectively. The variation of ultimate load intensity of GPHS with stiffness of geogrid is shown in Fig. 12. For floating GPHS, ultimate load intensity of granular piles increased marginally up to 80 kN/m stiffness and then became constant for higher stiffness. In floating GPHS, frictional stresses have not been mobilised significantly on the surface of geogrid strips when axial stiffness of geogrid increases. It may also due to the fact that floating granular piles with higher geogrid axial stiffness start penetrating into soft clay rather than deforming. For end bearing GPHS, ultimate load intensity of granular piles increased sharply up to 80 kN/m stiffness and then increased marginally for higher stiffness.

Numerical analysis has also been carried out to evaluate the improvement in the ultimate bearing capacity of granular piles treated ground when the entire cross section area is loaded. It represents actual field behaviour of an interior granular pile when large groups of piles are loaded simultaneously. Figure 13 presents FEM results in terms of load–settlement behaviour for end bearing GPHS. It may be noted that curves are almost linear up to 25 mm settlement. Therefore, load intensity (corresponding to 25 mm settlement) was considered as ultimate bearing capacity of improved ground. This settlement (25 mm) is about 14% of loading plate diameter. The ultimate bearing capacity of treated ground has been found to increase with a reduction in the vertical spacing of geogrid strips. The ultimate bearing capacity of 25, 50 and 70 mm c/c spaced end bearing GPHS-treated ground was found to increase by 122, 107 and 92%, respectively, as compared to untreated ground.

Deformation and failure mode

After completion of each test, aggregates were removed carefully and then slurry of plaster of Paris was poured into thus formed hole and allowed to set for 24 h. Surrounding clay was removed and deformed shape of granular piles was obtained and painted in white colour for better visibility of bulging. Deformed shapes were also obtained from PLAXIS 3D models. Figures 14(a–b) and 15(a–b) show deformed shape from laboratory model and FEM analysis for floating (URGP and GPHS) and end bearing (URGP and GPHS), respectively. It may be seen that the failure in URGP is mainly attributed to bulging due to poor lateral confinement. The depth of maximum bulging was observed to be in the range of 1–1.6d, from the top of pile. The total length of the URGP experiencing bulging was found to be in the range of 1.5–2.5d, from the top of pile. For floating GPHS, bulging is controlled due to confinement provided from horizontal geogrid strips. The floating GPHS with 70 mm spacing was observed to fail in bulging, whereas 25 and 50 mm spaced GPHS have been found to penetrate into clay as shown in Fig. 14(a–b).

Conclusions

In the present investigation, laboratory model tests as well as numerical analyses were carried out on 75 mm diameter URGPs and GPHS (floating and end bearing). The effect of length of reinforcement, shear strength of clay, geogrid stiffness

and strips spacing were studied. The vertical load–settlement plots of laboratory model tests were compared with those obtained from FEM analyses by PLAXIS 3D. The following conclusions can be drawn from the study:

(1) The ultimate load intensity of granular piles has been found to improve due to inclusion of horizontal geogrid strips. It shows further enhancement with the increase in the length of granular piles.
(2) End bearing URGPs can favourably be replaced by floating GPHS.
(3) The ultimate load intensity of GPHS (floating and end bearing) increases with the reduction in vertical spacing of geogrid strips.
(4) The ultimate load intensity of end bearing GPHS treated ground increases with an increase in the length of reinforcement.
(5) The ultimate load intensity of GPHS (floating and end bearing) increases linearly with an increase in the shear strength of clay.
(6) For floating GPHS, the ultimate load intensity is found to increase marginally up to 80 kN/m stiffness of geogrid, and then is constant for higher stiffness. The ultimate load intensity of end bearing GPHS increases up to 120 kN/m stiffness of geogrid, and then is constant for higher stiffness.
(7) The ultimate bearing capacity of end bearing GPHS-treated ground increases with a reduction in the spacing of geogrid strips.
(8) For URGP, the maximum depth and length of bulging lie in the range of 1–1.6d and 1.5–2.5d, respectively. For floating and end bearing GPHS, bulging is controlled due to confinement provided from horizontal geogrid strips.

References

Ali, K., Shahu, J. T. and Sharma, K. G. 2012. Model tests on geosynthetic-reinforced stone columns: a comparative study, *Geosynthetics International*, **19**, (4), 292–305.

Almeida, M., Hosseinpour, I., Ricci, M. and Alexiew, D. 2014. Behavior of geotextile-encased granular columns supporting test embankment on soft deposit, *Journal of Geotechnical and Geoenvironmental Engineering, ASCE*, **141**, (3), 1943-5606.0001256, 04014116.

Ambily, A. P. and Gandhi, S. R. 2007. Behavior of stone columns based on experimental and FEM analysis, *Journal of Geotechnical and Geoenvironmental Engineering, ASCE*, **133**, (4), 405–415.

ASTM D4595. 1986. Standard test method for tensile properties of geotextiles by the wide-width strip method, West Conshohocken, PA, ASTM International.

Ayadat, T., Hanna, A. M. and Hamitouche, A. 2008. Soil improvement by internally reinforced stone columns, Proceedings of the Institution of Civil Engineers - Ground Improvement, **161**, (2), 55–63.

Barksdale, R. D. and Bachus, R. C. 1983. Design and construction of stone columns, RD, 83/026, Federal Highway Administration, Washington, D.C.

Basu, P. 2009. Behaviour of sand-fibre mixed granular piles, Ph.d thesis, Indian Institute of Technology Roorkee, Roorkee, India.

Bowles, J. E. 1997. Foundation analysis and design, Singapore, Mc Graw Hill International Editions.

Chen, J. F., Li, L. Y., Xue, J. F. and Feng, S. Z. 2015. Failure mechanism of geosynthetic encased stone columns in soft soils under embankment, *Geotextiles and Geomembranes*, **43**, (5), 424–431.

Ghazavi, M. and Nazari Afshar, J. N. 2013. Bearing capacity of geosynthetic encased stone columns, *Geotextiles and Geomembranes*, **38**, 26–36.

Gniel, J. and Bouazza, A. 2009. Improvement of soft soils using geogrid encased granular columns, *Geotextiles and Geomembranes*, **27**, (3), 167–175.

Hasan, M. and Samadhiya, N. K. 2016. Experimental and numerical analysis of geosynthetic-reinforced floating granular piles in soft clays, *International Journal of Geosynthetics and Ground Engineering*, **2**, (22), 1–13. doi: 10.1007/s40891-016-0062-6

Hong, Y. S. and Wu, C. S. 2013. The performance of a sand column internally reinforced with horizontal reinforcement layers, *Geotextiles and Geomembranes*, **41**, 36–49.

Iai, S. 1989. Similitude for shaking table tests on soil-structure-fluid model in 1g gravitational field, *Soils and Foundations*, **29**, (1), 105–118.

IS: 1498. 2000. Classification and identification of soils for general engineering purposes, New Delhi, India, Indian Standards Institution.

Madhav, M. R. 1982. Recent development in the use and analysis of granular piles. Proceedings of Symposium on Recent Development in Ground Improvement Techniques, Bangkok, 117–129.

Madhav, M. R., Alamghir, M. and Miura, N. 1994. Improving granular column capacity by geogrid reinforcement. Proceedings of the 5th International Conference on Geotextiles, Geomembranes and Related Products, Singapore, 351–356.

Mitchell, J. K. and Huber, T. R. 1985. Performance of a stone column foundation, *Journal of Geotechnical and Geoenvironmental Engineering, ASCE*, **111**, (2), 205–223.

Mohanty, P. and Samanta, M. 2015. Experimental and numerical studies on response of the stone column in layered soil, *International Journal of Geosynthetics and Ground Engineering*, **1**, (27), 1–14.

Mohapatra, S. R., Rajagopal, K. and Sharma, J. 2016. Direct shear tests on geosynthetic-encased granular columns, *Geotextiles and Geomembranes*, **44**, 396–405.

Murugesan, S. and Rajagopal, K. 2006. Geosynthetic-encased stone columns: numerical evaluation, *Geotextiles and Geomembranes*, **24**, 349–358.

Murugesan, S. and Rajagopal, K. 2007. Model tests on geosynthetic-encased stone columns, *Geosynthetics International*, **24**, (6), 346–354.

Murugesan, S. and Rajagopal, K. 2010. Studies on the behavior of single and group of geosynthetic encased stone columns, *Journal of Geotechnical and Geoenvironmental Engineering*, **136**, (1), 129–139.

Ng, K. S. and Tan, S. A. 2015. Stress transfer mechanism in 2D and 3D unit cell models for stone column improved ground, *International Journal of Geosynthetics and Ground Engineering*, **1**, (3), 1–9.

Pulko, B., Majes, B. and Logar, J. 2011. Geosynthetic-encased stone columns: analytical calculation model, *Geotextiles and Geomembranes*, **29**, (1), 29–39.

Samadhiya, N. K., Maheswari, P., Basu, P. and Kumar, M. B. 2008. Load settlement characteristics of granular piles with randomly mixed fibres, *Indian Geotechnical Journal*, **38**, (3), 345–354.

Sharma, R. S., Kumar, B. R. P. and Nagendra, G. 2004. Compressive load response of granular piles reinforced with geogrids, *Canadian Geotechnical Journal*, **41**, (1), 187–192.

Wu, C. S. and Hong, Y. S. 2008. The behavior of a laminated reinforced granular column, *Geotextiles and Geomembranes*, **26**, (4), 302–316.

Wu, C. S. and Hong, Y. S. 2009. Laboratory tests on geosynthetic encapsulated sand columns, *Geotextiles and Geomembranes*, **27**, 107–120.

Yoo, C. and Lee, D. 2012. Performance of geogrid-encased stone columns in soft ground: full-scale load tests, *Geosynthetics International*, **19**, (6), 480–490.

Zhang, L. and Zhao, M. 2015. Deformation analysis of geotextile-encased stone columns, *International Journal of Geomechanics*, **15**, (3), 04014053.